Protein-Polyelectrolyte Cluster Formation and Redissolution:
A Monte Carlo Study

Fredrik Carlsson,*,† Martin Malmsten,†,‡ and Per Linse§

*Contribution from the Institute for Surface Chemistry, Box 5607,
SE−114 86 Stockholm, Sweden, Department of Chemistry, Surface Chemistry, Royal Institute of
Technology, SE−100 44 Stockholm, Sweden, and Physical Chemistry 1, Center for Chemistry
and Chemical Engineering, Lund University, Box 124, SE−221 00 Lund, Sweden*

Received July 8, 2002 ; E-mail: fredrik.carlsson@alliedchem.se

Abstract: Aqueous solutions of proteins and oppositely charged polyelectrolytes were studied at different
polyelectrolyte chain length, ionic strength, and protein−protein interaction potential as a function of the
polyelectrolyte concentration. One of the protein models used represented lysozyme in aqueous environment.
The model systems were solved by Monte Carlo simulations, and their properties were analyzed in terms
of radial distribution functions, structure factors, and cluster composition probabilities. In the system with
the strongest electrostatic protein−polyelectrolyte interaction the largest clusters were formed near or at
equivalent amount of net protein charge and polyelectrolyte charge, whereas in excess of polyelectrolyte
a redissolution appeared. Shorter polyelectrolyte chains and increased ionic strength lead to weaker cluster
formation. An inclusion of nonelectrostatic protein−protein attraction promoted the protein−polyelectrolyte
cluster formation.

1. Introduction

Protein−polyelectrolyte interactions are important in a variety of contexts such as protein purification,[1] drug delivery systems,[2] and food technology,[3] and several review articles are availabe.[4−6] It has been known for a long time that addition of a polyelectrolyte to a protein solution can lead to the formation of protein−polyelectrolyte complexes and larger clusters and eventually to a coacervate and precipitation. Moreover, the reverse process may appear upon further addition of polyelectrolyte,[7,8] in the following referred to as redissolution. This behavior is analogous to the precipitation and the subsequent redissolution appearing in other systems containing charged latex particles,[9,10] silica particles,[11] or bacteria[12,13] with oppositely charged polyelectrolytes as well as in water purification.[14]

Numerous investigations involving numerical simulations of charged particles with a central charge and oppositely charged polyelectrolytes have recently been performed. For instance, Granfeldt et al. examined the interaction between two charged spheres with polyelectrolyte between and found that the potential energy could be separated into an attractive term due to bridging and electrostatic correlations and a repulsive term of entropic origin.[15] Dickinson studied particles and polymers interacting with a square well potential and found either bridging flocculation or depletion flocculation depending on the interaction potential,[16] and thereafter Dickinson and Euston investigated the structure of flocs consisting of particles and polymers.[17,18] Moreover, Wallin and Linse considered charged hard spheres and flexible polyelectrolytes and the effects of chain flexibility, linear charge density of the chain, and particle radius on the free energy of complexation.[19−22] In addition, Nguyen and Shklovskii studied overcharging of spheres with polyelectrolytes,[23] and Chodanovski and Stoll studied the structure of the adsorbed polymer layer on the spheres as a function of the chain length and sphere radius at different ionic strength.[24,25]

† Institute for Surface Chemistry.
‡ Department of Chemistry, Surface Chemistry, Royal Institute of Technology.
§ Physical Chemistry 1, Center for Chemistry and Chemical Engineering, Lund University.

(1) Dubin, P. L.; Gao, J.; Mattison, K. *Sep. Purif. Methods* **1994**, *23*, 1−16.
(2) Malmsten, M. *Surfactants and Polymers in Drug Delivery*; Marcel Dekker: New York, 2002.
(3) Tolstoguzov, V. B. *Food Hydrocolloids* **1991**, *4*, 429−468.
(4) Dickinson, E.; Eriksson, L. *Adv. Colloid Interface Sci.* **1991**, *34*, 1−29.
(5) Xia, J.; Dubin, P. L. In *Macromolecular Complexes in Chemistry and Biology*; Dubin, Bock, Davis, Schulz, Thies, Eds.; Springer-Verlag: Berlin, 1994; pp 247−271.
(6) Tribet, C. In *Physical Chemistry of Polyelectrolytes*; Radeva, T., Ed.; Marcel Dekker: New York, 2001; Vol. 99, pp 687−741.
(7) Morawetz, H.; Walter L. Hughes, J. *J. Phys. Chem.* **1952**, *56*, 64−69.
(8) Berdick, M.; Morawetz, H. *J. Biol. Chem.* **1953**, *206*, 959−971.
(9) Eriksson, L.; Alm, B. In *Chemical Water and Wastewater Treatment II*; Klute, R., Hahn, H. H., Eds.; Springer-Verlag: Berlin, 1992; pp 19−32.
(10) Eriksson, L.; Alm, B.; Stenius, P. *Colloids Surf. A: Physicochem. Eng. Aspects* **1993**, *70*, 47−60.
(11) Wang, T. K.; Audebert, R. *J. Colloid Interface Sci.* **1986**, *119*, 459−456.
(12) Treweek, G. P.; Morgan, J. J. *J. Colloid Interface Sci.* **1977**, *60*, 258−273.

(13) Eriksson, L. B.; Härdin, A.-M. In *Flocculation in Biotechnology and Separation Systems*; Attia, Y. A., Ed.; Elsevier Science Publishers B. V.: Amsterdam, 1987; pp 441−455.
(14) Eriksson, L.; Alm, B. *Wat. Sci. Technol.* **1993**, *28*, 203−212.
(15) Granfeldt, M. K.; Jönsson, B.; Woodward, C. E. *J. Phys. Chem.* **1991**, *95*, 4819−4826.
(16) Dickinson, E. *J. Colloid Interface Sci.* **1989**, *132*, 274−278.
(17) Dickinson, E.; Euston, S. R. *J. Chem. Soc., Faraday Trans.* **1991**, *87*, 2193−2199.
(18) Dickinson, E.; Euston, S. R. *Colloids Surf.* **1992**, *62*, 231−242.
(19) Wallin, T.; Linse, P. *J. Phys. Chem.* **1996**, *100*, 17 873−17 880.
(20) Wallin, T.; Linse, P. *Langmuir* **1996**, *12*, 305−314.
(21) Wallin, T.; Linse, P. *J. Phys. Chem.* **1997**, *101*, 5506−5513.
(22) Wallin, T.; Linse, P. *J. Chem. Phys.* **1998**, *109*, 5089−5100.
(23) Nguyen, T. T.; Shklovskii, B. I. *J. Chem. Phys.* **2001**, *114*, 5905−5916.

Table 1. Parameters Used in the Simulations

parameter	value	parameter	value
N_{bead}	30 or 60	k_{bond}	2.4 kJ/mol/Å^2
N_{prot}	30	α_0	180°
Z_{bead}	−1	k_{ang}	0.0048 kJ/mol/(°)^2
Z_{prot}	+10	$\epsilon_{prot,prot}$	0 or 8.4 × 10^9 kJ/(mol Å^6)
R_{bead}	2.0 Å	T	298 K
R_{prot}	18.54 Å	ϵ_r	78.4
r_0	4.7 Å	L_{box}	400 Å

Akinchina and Linse examined the structure of complexes formed at different chain flexibility[26] and Jonsson and Linse the effects of the linear charge density of the chain, the chain length, the macroion charge[27] and the effects of the chain flexibility[28] on the complexation between macroions and polyelectrolytes in solution. Finally, the phase stability of solutions containing charged particles and oppositely charged polyelectrolytes has theoretically been considered by, e.g., Jiang and Prausnitz[29] and Nguyen and Shklovskii.[30]

Previously, we have investigated the self-association of lysozyme in solution and the complexation between one lysozyme and one oppositely charged polyelectrolyte in solution employing Monte Carlo simulations.[31,32] Particular emphasis was made on the role of electrostatic interactions, and for this purpose a protein model taking into account the discrete charges of lysozyme was developed.

In the present work, we extend our studies on protein–polyelectrolyte cluster formation to include systems representing protein solutions at variable polyelectrolyte concentration. The focus is on the effects of the system composition on the formation of protein–polyelectrolyte clusters for different polyelectrolyte length, ionic strength, and protein–protein interaction potential. In particular, aspects related to cluster composition and charge matching are examined.

2. Model

A simple model taking into account (i) excluded volume effects of the protein and the polymer, (ii) polymer connectivity and flexibility, (iii) electrostatic interactions using a screened Coulomb potential, and (iv) hydrophobic interactions between the proteins have been employed. Water enters the model only through its dielectric permittivity. Recent comparisons using results from more elaborated models containing explicit simple ions have shown that the screened Coulomb potential is a reasonable simplification for describing the complexation between oppositely charged macromolecules at low ionic strength.[33,34]

With the interactions taken to be pairwise additive, the total potential energy of the system U_{tot} becomes

$$U_{tot} = U_{bond} + U_{ang} + U_{nonbond} \quad (1)$$

where U_{bond}, U_{ang}, and $U_{nonbond}$ denote the bond potential energy, the angular potential energy of the polyelectrolyte, and all nonbonded potential energy between the particles, respectively.

2.1 Polyelectrolyte. The polyelectrolyte is modeled as a chain of hard spheres, each holding one negative elementary charge in the center. Harmonic bonds join the hard spheres and a harmonic angular term regulates the intrinsic flexibility of

the chains. The polyelectrolyte bond and angular potential energy terms are given by

$$U_{bond} = \sum_{i=1}^{N_{bead}-1} \frac{k_{bond}}{2}(r_{i,i+1} - r_0)^2 \quad (2)$$

and

$$U_{ang} = \sum_{i=2}^{N_{bead}-1} \frac{k_{ang}}{2}(\alpha_i - \alpha_0)^2 \quad (3)$$

respectively. In eq 2, $r_{i,i+1}$ denotes the center to center-to-center distance between the polyelectrolyte bead i and $i+1$, r_0 the equilibrium separation of the bond potential, and k_{bond} the bond force constant. In eq 3, α_i denotes the angle formed by the vectors $\mathbf{r}_{i+1}$- $\mathbf{r}_i$ and $\mathbf{r}_{i-1}$- $\mathbf{r}_i$, α_0 the equilibrium angle of the harmonic potential, and k_{ang} the angular force constant. The values of these parameters are collected in Table 1. The flexibility of the chain regulated by k_{ang} is adjusted so that the bare persistence length (the persistence length without electrostatic interactions) becomes $\approx$ 35 Å.[26]

2.2 Protein. The protein is modeled as a hard sphere with radius R_{prot} = 18.54 Å with embedded charges representing charges of ionized amino acids. The number of positive and negative charges at a given pH is based on the pK_a values of all titrating amino acids of lysozyme.[35] The charges were positioned 2.0 Å beneath the hard sphere surface, providing a minimum charge–charge distance representing the size of a hydrated charge in aqueous solution. The positions of the charges are based on their coordinates from the lysozyme crystal structure,[36] and the construction of this model was described in detail elsewhere.[31] The structure of protein is held fixed and independent of its degree of complexation. Experimental data from circular dicroism studies on lysozyme in solutions and in complexes with oppositely charged copolymers[37] show that lysozyme preserve its gross structure, making our assumption reasonable. Moreover, the protein net charge Z_{prot} was also assumed to be independent of the complexation and ionic strength. The more simplified approach of representing the protein charge distribution with a single charge at the center of the protein leads to a less attractive electrostatic interaction between the protein and an oppositely charge polyelectrolyte.[31]

2.3 Nonbonded Interactions. The nonbonded potential energy is given by

$$U_{nonbond} = U_{hs} + U_{el} + U_{short} \quad (4)$$

where the hard sphere repulsion is given by

(24) Chodanowski, P.; Stoll, S. *J. Chem. Phys.* **2001**, *115*, 4951−4960.
(25) Chodanowski, P.; Stoll, S. *Macromolecules* **2001**, *34*, 2320−2328.
(26) Akinchina, A.; Linse, P. *Macromolecules* **2002**, *35*, 5183−5193.
(27) Jonsson, M.; Linse, P. *J. Chem. Phys.* **2001**, *115*, 3406−3418.
(28) Jonsson, M.; Linse, P. *J. Chem. Phys.* **2001**, *115*, 10975−10985.
(29) Jiang, J.; Prausnitz, J. M. *J. Phys. Chem. B* **1999**, *103*, 5560−5569.
(30) Nguyen, T. T.; Shklovskii, B. I. *J. Chem. Phys.* **2001**, *115*, 7298−7308.
(31) Carlsson, F.; Linse, P.; Malmsten, M. *J. Phys. Chem. B* **2001**, *105*, 9040−9049.
(32) Carlsson, F.; Malmsten, M.; Linse, P. *J. Phys. Chem. B* **2001**, *105*, 12 189−12 195.
(33) Hayashi, Y.; Ullner, M.; Linse, P. *J. Phys. Chem* **2002**, *116*, 6836−6845.
(34) Skepö, M.; Linse, P. *Phys. Rev. E* **2002**, *66*, 051807-1−051807-7.
(35) Kuramitsu, S.; Hamaguchi, K. *J. Biochem.* **1980**, *87*, 1215−1219.
(36) Ramanadham, M.; Sieker, L. C.; Jensen, L. H. *Acta Crystallogr. B* **1990**, *B46*, 63−69.
(37) Harada, A. *Journal of Controlled Release* **2001**, *72*, 85−91.

$$U_{hs} = \sum_{i<j} u_{ij}^{hs}(r_{ij}) \quad (5)$$

$$u_{ij}^{hs}(r_{ij}) = \begin{cases} 0 & r_{ij} \geq (R_i + R_j) \\ \infty & r_{ij} < (R_i + R_j) \end{cases} \quad (6)$$

with the summation in eq 5 extending over the protein centers and chain beads. The screened electrostatic interaction is given by

$$U_{el} = \sum_{i<j} \frac{Z_i Z_j e^2}{4\pi\epsilon_0 \epsilon_r} \frac{1}{r_{ij}} \exp(-\kappa r_{ij}) \quad (7)$$

with the summation extending over all charges. Finally, the attractive nonelectrostatic protein−protein potential energy

$$U_{short} = -\sum_{i<j} \frac{\epsilon_{prot,prot}}{r_{ij}^6} \quad (8)$$

was used with the summation extending over protein centers and $\epsilon_{prot,prot}$ (≥ 0) a parameter controlling the magnitude of the nonelectrostatic attraction. Moreover, r_{ij} denotes the center-to-center distance between particles i and j, Z_i the charge of site i, ϵ_0 the permittivity of vacuum, ϵ_r the relative permittivity of the solvent, $\kappa = [(1/\epsilon_0\epsilon_r kT) \sum_m (Z_m e)^2 c_m]^{1/2}$ the inverse Debye screening length with c_m being the bulk concentration of salt species m including the counterions of the charged macroions. The salt content is given in terms of the ionic strength, $I = 0.5\sum_m Z_m^2 c_m$, and at the conditions used $I = 0.1$ M corresponds to $\kappa^{-1} = 9.6$ Å. Values of these parameters used are also collected in Table 1.

2.4 Systems. Four different systems were considered at different polyelectrolyte concentrations, see Table 2. In all systems, the protein carried a net charge $Z_{prot} = +10$ (corresponding to pH ≈ 4.5) originating from 19 positive and 9 negative charges and the simulated box contained $N_{prot} = 30$ proteins. System 1 is characterized by no nonelectrostatic protein−protein attraction ($\epsilon_{prot,prot} = 0$), low ionic strength ($I = 0.01$ M), and relatively long polyelectrolyte chains ($N_{chain} = 60$), whereas system 2 possesses shorter polyelectrolyte chains ($N_{chain} = 30$) and system 3 a higher ionic strength ($I = 0.1$ M). In system 4, a nonelectrostatic attraction between the proteins was added ($\epsilon_{prot,prot} > 0$). The value of $\epsilon_{prot,prot}$ was chosen such that calculated second virial coefficients B_{22} of model protein solutions fits corresponding experimental data[38] of lysozyme solutions. This was described in detail in an earlier study by us.[32]

Thus, in systems 1−3 the model protein has a charge distribution representing lysozyme at pH ≈ 4.5, but the proteins interact only with hard-sphere repulsion and electrostatic forces, and comparisons among these systems will provide information on the role of the polyelectrolyte length and ionic strength. In system 4, the additional nonelectrostatic protein−protein interaction make the model protein representing lysozyme, and the comparison of results pertaining systems 3 and 4 will illustrate the effects of a nonelectrostatic protein−protein relevant for lysozyme in water.

(38) Velev, O. D.; Kaler, E. W.; Lenhoff, A. M. *Biophys. J.* **1998**, *75*, 2682−2697.

Table 2. Overview of the Systems Examined

system	$\epsilon_{prot,prot}$ (kJ/(mol Å⁶))	I (M)	N_{bead}	N_{chain}[a]
1	0	0.01	60	0, 1, 4, 5, 6, 10, 20
2	0	0.01	30	0, 2, 8, 10, 12, 20, 40
3	0	0.1	60	0, 1, 4, 5, 6, 10, 20
4	8.4×10^9	0.1	60	0, 1, 4, 5, 6, 10, 20

[a] These values corresponds to $\beta = 0, 0.2, 0.8, 1, 1.2, 2,$ and 4, respectively.

In the following, the stoichiometric charge ratio $\beta = (N_{chain}N_{bead}|Z_{bead}|)/(N_{prot}|Z_{prot}|)$ involving the charge of all polyelectrolyte beads $N_{chain}N_{bead}Z_{bead}$ and the net charge of all proteins $N_{prot}Z_{prot}$ in the solution will be used to describe the different polyelectrolyte concentrations. All systems have been examined at 7 different polyelectrolyte concentrations covering β from 0 to 4, see Table 2.

3. Method

3.1 Simulation Details. The model systems were solved by Metropolis Monte Carlo simulations at constant number of particles, constant volume, and constant temperature. The particles were enclosed in a cubic box with box length $L_{box} = 400$ Å. Periodic boundary conditions were applied in all three directions, and the interactions were truncated at $R_{cut} = L_{box}/2$.

Two different types of moves were employed during the simulation: (i) single particle moves of all particles sampled uniformly in the interval $[-\Delta_i/2, \Delta_i/2]$ and (ii) rotation of the proteins with an angle sampled uniformly in the interval $[-\theta_i/2, \theta_i/2]$ with $\theta_{prot} = 360°$ around a selected axis. Δ_{prot} was adjusted for each system and was 1.0−7.0 Å, smaller for larger number of chains and lower ionic strength, providing an acceptance ratio of about 50%. Δ_{bead} was 2.0 Å throughout. The equilibrations involved at least 0.1×10^6 passes (attempted moves per particle) and they were followed by production simulations comprising 1×10^6 passes. The statistical error was based on a division of the simulation into 10 sub-batches. All simulations were carried out using the integrated Monte Carlo/molecular dynamics/Brownian dynamics simulation package Molsim.[39]

3.2. Cluster Criterion. Clusters containing oppositely charged proteins and polyelectrolytes were expected to form, and the appearance of such clusters and their compositions were analyzed. Two macromolecules (protein or polyelectrolyte) were considered to belong to the same cluster if they were "connected" directly or indirectly through one or several other macromolecules. Two proteins were directly connected if $r_{prot,prot} \leq 2R_{prot} + \Delta_{cluster}$, a protein and a polyelectrolyte were directly connected if $r_{prot,bead} \leq R_{prot} + R_{bead} + \Delta_{cluster}$ for at least one bead, whereas two polyelectrolytes were directly connected if $r_{bead,bead} \leq 2R_{bead} + \Delta_{cluster}$ for at least one bead-bead pair. Here, $\Delta_{cluster} = 5$ Å was used, but the trends observed are not sensitive on the exact value of $\Delta_{cluster}$.

3.3 Ergodicity. Because the complexation between a protein and an oppositely charged polyelectrolyte may be strong, it is important to consider the ergodicity of the simulations. Therefore, several different quantities assessing the ergodicity have been employed. In the following, data for primarily system 1

(39) Linse, P.; Wallqvist, A.; Åstrand, P.-O.; Nymand, T. M.; Lobaskin, V.; Carlsson, F. In; MOLSIM, Version 3.2: Lund University, Sweden, 2001.
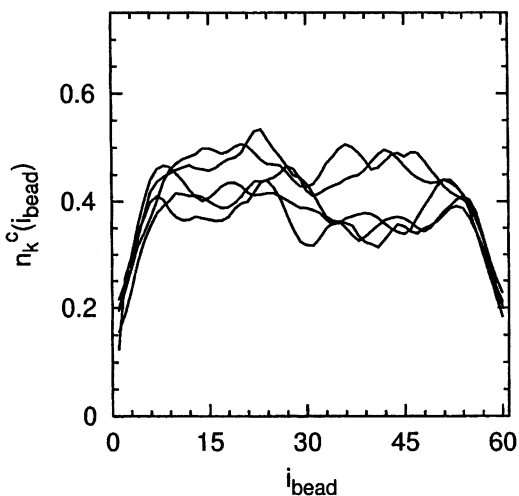
Figure 1. Complexation function $n_k^c(i_{bead})$ denoting the average number of proteins complexed to bead i_{bead} in a polyelectrolyte chain. The functions are plotted for each of the 5 polyelectrolyte chains in system 1 with $\beta = 1$.

with the strongest cluster formation (long polyelectrolyte chains and low ionic strength) will be discussed.

Consider first the probability that bead i_{bead} in chain k is complexed to protein j, $P_{k,j}^c(i_{bead})$. One protein and one polyelectrolyte are here considered as complexed if there are directly connected according to the cluster definition. Such complexation functions have previously been employed to characterize the complexation between one polyelectrolyte and one protein.[31] In system 1 at $\beta = 1$, the set $\{P_{k,j}^c(i_{bead}), k = 1$ to $N_{chain}, j = 1$ to $N_{prot}\}$ shows that a given protein form a complex with all the five polyelectrolyte during the simulation (data not shown). Thus, proteins are complexed with different polyelectrolytes during different stages of the simulations. We have also considered the average number of proteins complexed with i_{bead} in chain k according to $n_k^c(i_{bead}) = \sum_{j=1}^{N_{prot}} P_{k,j}^c(i_{bead})$. Figure 1 shows $n_k^c(i_{bead})$ for the five different polyelectrolytes at $\beta = 1$, and it is seen that all $n_k^c(i_{bead})$ are reasonable symmetric at $i_{bead} = (N_{bead}+1)/2$ and that the number of proteins complexing the different chains are approximately equal. Thus, on the average all chains experience the same degree of complexation and are equivalent.

Moreover, the root-mean-square (rms) displacements of protein and polyelectrolyte beads during the simulations were monitored and found to be between 70 and 170 Å for proteins and between 130 and 4100 Å for polyelectrolyte beads across the different systems and polyelectrolyte concentrations. From an examination of the displacements of individual proteins, it was found that all proteins were subjected to similar displacements during the simulation, i.e., no protein was found to be trapped during the simulations. Thus, based on these findings, we conclude that all simulations were ergodic in practice.

4. Results and Discussion

We will now present data on the properties of the protein-polyelectrolyte solutions for the different systems at different polyelectrolyte concentrations. As already alluded to, the strong protein−polyelectrolyte attraction dominates the properties of these systems. This is illustrated in Figure 2, which shows configurations from the simulations of system 1 with charge ratios $\beta = 0$, 1, and 4. At $\beta = 0$ (top panel), corresponding to
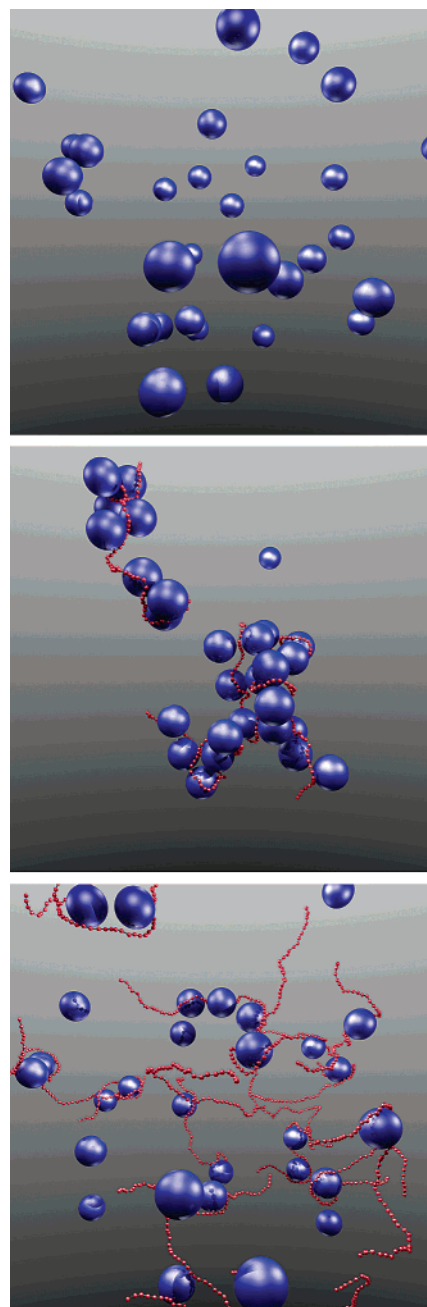

Figure 2. Snapshot from the simulations of system 1 with $\beta = 0$, 1, and 4 (top to bottom) displaying positively net charged proteins (blue spheres) and negatively charged polyelectrolyte beads (red spheres). For clarity the discrete protein charges are not shown.

a polyelectrolyte-free protein solution, the proteins are well separated and hence effective repulsions are operating between the proteins. However, in the snapshot at $\beta = 1$ (middle panel), corresponding to an equal amount of net protein charge and polyelectrolyte charge, protein clusters held together by extended chains are formed. As mentioned in the previous section, these clusters are reshaped during the simulation and thus represent equilibrium structures of the model system. Finally, at $\beta = 4$ (bottom panel) with a 4-fold excess of polyelectrolyte charges, the large clusters are redissolved and the proteins are to a large extent again separated from each other. However, the proteins are still complexed to the polyelectrolytes.

4.1 Cluster Formation and Redissolution. The formation of clusters and the subsequent redissolution in the protein−

polyelectrolyte systems will now quantitatively be described by considering structure properties as radial distribution functions (rdf's) and structure factors (sf's). The radial distribution function $g_{ij}(r)$ expresses the relative density of a particle of type j at a distance r from a given particle of type i. At short distance $g_{ij}(r)$ is zero because of hard-sphere overlap, whereas in a homogeneous solution $g_{ij}(r)$ conventionally approaches unity at large r. The partial structure factor $s_{ij}(q)$ is essentially the Fourier transformation of $g_{ij}(r)$ and provides the same information, although emphasising different aspects. In particular, $s(q)$ at small q provides information on the compressibility and hence on the stability of the system. Because the systems are investigated at fixed number of proteins with variable amount of polyelectrolyte, we focus on the protein−protein pair of the three distinct pairs available. Moreover, the protein−polyelectrolyte and the polyelectrolyte−polyelectrolyte rdf's and the corresponding partial sf's provide similar picture of the cluster formation owing to the electrostatic coupling in the systems.

Figure 3 provides the protein−protein rdf's of the four systems considered at different amount of polyelectrolyte added. The arrows illustrate the order of increasing polyelectrolyte concentration. The corresponding structure factors are given by the inserts.

4.1.1 System 1. Starting with system 1, Figure 3a shows that for a polyelectrolyte-free protein solution ($\beta = 0$), $g_{prot,prot}(r)$ is zero at hard-sphere contact, increases smoothly as r is increased, and approaches unity at $r \approx 100$ Å. Thus, the electrostatic repulsion keeps the proteins apart and creates a homogeneous solution as seen in Figure 2, top. When polyelectrolyte is added ($\beta > 0$), the magnitude of $g_{prot,prot}(r)$ at $r \leq 100$ Å increases until approximately charge equivalence ($\beta = 1$) is achieved. At $\beta = 1$, $g_{prot,prot}(r)$ displays a large and broad peak at short protein−protein separation, hence verifying the cluster formation shown in Figure 2, middle. At excess polyelectrolyte charge ($\beta > 1$), the magnitude of $g_{prot,prot}(r)$ at short r decreases, and at a 4-fold excess of polyelectrolyte charge ($\beta = 4$) the magnitude has fallen below that at $\beta = 0.2$. Nevertheless, $g_{prot,prot}(r)$ differs still qualitatively from that in polyelectrolyte-free protein solution and displays an enhanced density of proteins near a given protein. Thus, at $\beta = 4$ an increased probability of forming protein pairs mediated by polyelectrolyte chains appears (cf. Figure 2, bottom and top).

In more detail, the magnitude of the peak at short separation is slightly *larger* for both $\beta = 0.8$ and 1.2 as compared to $\beta = 1$, and hence, the maximum cluster formation occurs slightly off $\beta = 1$. In a related simulation study on the complexation in solution of oppositely charged polyelectrolytes of equal absolute charge,[40] it was found that the formation of the largest clusters occurred slightly off charge equivalence and in agreement with our results. In that study, is was concluded that at the charge ratio $\beta = 1$ large neutral clusters display a tendency to separate into smaller clusters, whereas slightly off charge equivalence such a division of charged clusters was less probable since a smaller cluster with the same net charge as the original one would be formed. Generally, it is favorable to distribute excess charges in a large cluster.[40]

Moreover, the broad peak between $2R_{prot} \approx 37$ and 60 Å display two maximums, one at $r = 2R_{prot}$ and one at r ≈ 45 Å. The former maximum corresponds to two proteins being in hard-
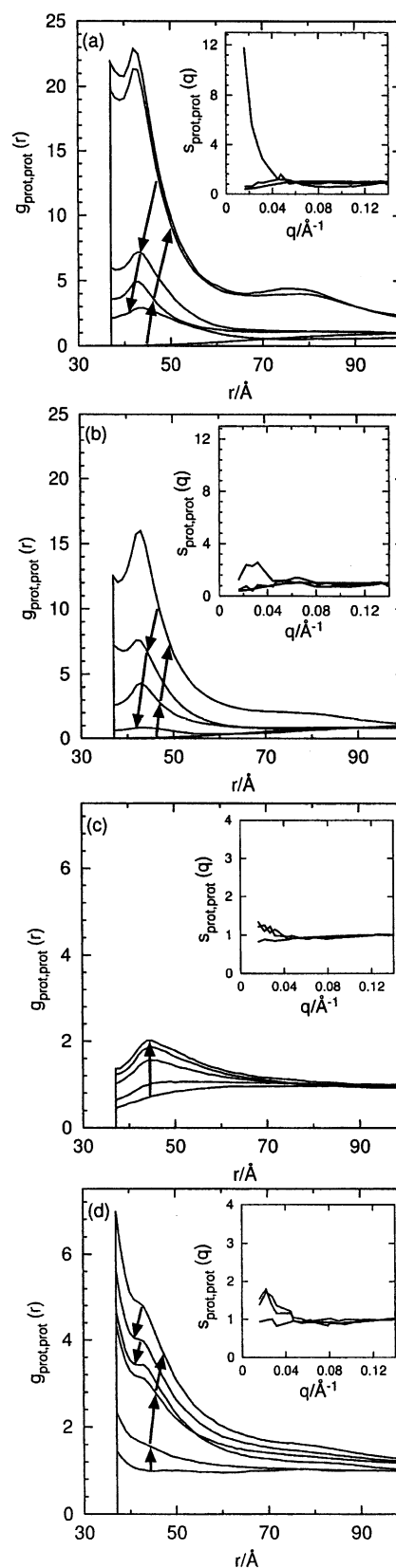

Figure 3. Protein-protein radial distribution function $g_{prot,prot}(r)$ for (a) system 1 with $\beta = 1.2$, 1, 2, 0.2, 4, and 0 (top to bottom); (b) system 2 with $\beta = 0.8$, 2, 0.2, 4, and 0 (top to bottom); (c) system 3 with $\beta = 4$, 2, 0.8, 0.2, and 0 (top to bottom); (d) system 4 with $\beta = 1.2$, 2, 4, 0.8, 0.2, and 0 (top to bottom). Some of the simulated rdf's are omitted for clarity. The arrows illustrate the order of increasing polyelectrolyte concentration. The inserts show the protein−protein structure factors $s_{prot,prot}(q)$ for $\beta = 0$ (bottom), 1 (top), and 4.

(40) Hayashi, Y.; Ullner, M.; Linse, P. *J. Phys. Chem. B* **2002**, submitted.

sphere contact with each other, whereas the latter most likely to two nearby proteins separated by polyelectrolyte beads as seen in Figure 2, middle.

Finally, close to the charge ratio $\beta = 1$ an additional broad maximum appears at $r \approx 80$ Å, implying the appearance of a high density of next-nearest neighbors and supporting the notion of the formation of larger clusters. A verification of the appearance of large clusters is manifested by the protein−protein structure factor given in the insert of Figure 3a, displaying a sharp increase at small wave vector at $\beta = 1$. Also at $\beta = 0.8$ and 1.2 the structure factor displays a sharp increase at small wave vectors (data not shown). The maximal value of $s_{prot,prot}(q)$ for the present finite system is $N_{prot} = 30$.

Thus, at $\beta \approx 1$ extensive cluster formation appears, and in the thermodynamic limit the present system has the potential to display a phase separation, and hence showing the sequence (i) stable solution, (ii) unstable solution, and (iii) stable solution (redissolution) as the polyelectrolyte concentration is increased. However, an analysis of the cluster formation and structure factor at increasing system size is needed to support that conjecture. Nevertheless, the observed appearance as β is increased is in line with experimentally observed coacervate formation and redissolution, found in many different systems with charged particles and oppositely charged polyelectrolytes.[8,41] In a related simulation study involving polyelectrolytes and oppositely charged macroions *without* added salt,[42] a more decisive solution instability was found, which moreover persisted over a large variation of the density of the charged macromolecules, also in qualitative agreement with experimental results.

4.1.2 System 2. The corresponding behavior as shorter polyelectrolyte chains are added to the *same* initial protein solution is given in Figure 3b. Again the magnitude of $g_{prot,prot}(r)$ at short protein−protein separation is strongly increased, displays a maximum at $\beta \approx 1$, and reduces at larger β. Hence, the principal behavior is the same. However, the amplitude of the rdf at short r is smaller and the second maximum appearing at $r \approx 80$ Å is less pronounced as compared to system 1. Moreover, at $\beta \approx 1$ the protein−protein structure factor shown in the insert of Figure 3b displays a maximum $q \approx 0.03$ Å indicating the appearance of several separated clusters rather than a few large ones.

Thus, the ability of the oppositely charged polyelectrolyte to bring proteins together is substantially reduced as the chains are reduced from 60 to 30 beads, corresponding to a reduction of the charge ratio $N_{bead}|Z_{bead}|/|Z_{prot}|$ from 6 to 3. In particular, at $\beta \approx 1$ the shorter and less charged chains are less potent to form large clusters. Again, our observations are in qualitative agreement with experimental observations that longer polyelectrolyte gives rise to larger protein-polyelectrolyte clusters.[43]

4.1.3 System 3. Figure 3c shows the same scenario as for system 1, but at the higher ionic strength $I = 0.1$ M. In the polyelectrolyte-free solution, $g_{prot,prot}(r)$ displays a considerable contact value, showing that the larger electrolyte concentration now considerably screens the electrostatic protein−protein repulsion appearing in system 1. As polyelectrolyte is added, $g_{prot,prot}(r)$ at short r increases *continuously* as β is increased to $\beta = 4$. Thus, there is no optimum at $\beta \approx 1$ as observed at the

lower ionic strength. Moreover, the rise of the rdf is only very moderate and no second peak at larger separation appears. Hence, we conclude that there is only a weak enhancement of finding pairs of proteins mediated by the polyelectrolyte chains at all polyelectrolyte concentrations considered. Obviously, at $I = 0.1$ M the electrostatic attraction between proteins and polyelectrolyte chains is too weak to form more extended clusters. (It should however be noted that the screened Coulomb potential used, eq 7, exaggerate the screening effect of the electrolyte, because the hard-sphere nature of the protein and the beads to exclude screening electrolyte is not taken into account. Thus, the reduced tendency of complex formation displayed as the ionic strength is increased is most likely overestimated).

4.1.4 System 4. The structure of system 4 is provided in Figure 3d at different polyelectrolyte concentrations. System 4 differs from system 3 by the existence of a nonelectrostatic protein attraction. A comparison between Figures 3c and 3d shows that the protein density near a protein in a polyelectrolyte-free solution ($\beta = 0$) is enhanced by the nonelectrostatic attraction. In system 4, $g_{prot,prot}(r)$ displays a maximum at hard-sphere contact demonstrating that the weak electrostatic repulsion appearing in system 3 is now counteracted by the nonelectrostatic attraction. This appearance of an oligomerization in a pure protein solution was examined previously.[32] As polyelectrolytes are added, $g_{prot,prot}(r)$ for system 4 displays a *different* behavior as compared to system 3, but the same qualitative changes as in systems 1 and 2, i.e., an increase of $g_{prot,prot}(r)$ at short separation up to $\beta \approx 1$ and a decline at larger β. The raise of $g_{prot,prot}(r)$ at short r is however smaller than in systems 1 and 2, indicating a smaller tendency of forming clusters and the magnitude of the protein−protein structure factor at short wave vectors is also modest. Figure 3d also shows that the maximal value of $g_{prot,prot}(r)$ at $\beta > 1$ appears at protein contact. Only a shoulder at $r \approx 45$ Å remains of the second maximum of the splitted peak in systems 1 and 2. This shift from polyelectrolyte separated protein pairs to direct protein hard-sphere contacts is of course a consequence of the nonelectrostatic protein−protein attraction.

Hence, the inclusion of a nonelectrostatic attraction between charged proteins promotes the formation of clusters upon addition of oppositely charged polyelectrolytes. This cluster formation is obviously possible *even* if the system without the nonelectrostatic attraction does not display an extensive cluster formation. We envision that, whereas the electrostatic interactions are too screened to establish clusters in the absence of the nonelectrostatic attraction, the still rather weak increased probability to form protein pairs, originating from the nonelectrostatic attraction, facilitate the cluster formation. Now the electrostatic interaction between pairs of proteins and a polyelectrolyte becomes sufficiently strong the create clusters.

4.2 Cluster Composition. In the following, we will consider the probability of finding a cluster with n_{chain} polyelectrolyte chains and n_{prot} proteins, denoted by $P(n_{chain}, n_{prot})$. The probabilities $P(n_{chain}, n_{prot})$ was constructed by sampling the frequency at which clusters of different composition appeared during the simulations using the cluster criterion described in the Method section and are normalization according to $\sum_{nchain} \sum_{nprot} P(n_{chain}, n_{prot}) = 1$. Note, the probability of finding a macromolecule in a cluster of a given composition is a

(41) Eriksson, L. Thesis; Lund University: Lund, 1997.
(42) Skepö, M.; Linse, P. *Macromolecules* **2003**, *36*, 508−519.
(43) Shieh, J.-y.; Glatz, C. E. In *Macromolecular Complexes in Chemistry and Biology*; Dubin, P., et al., Eds.; Springer-Verlag: Berlin, 1994.
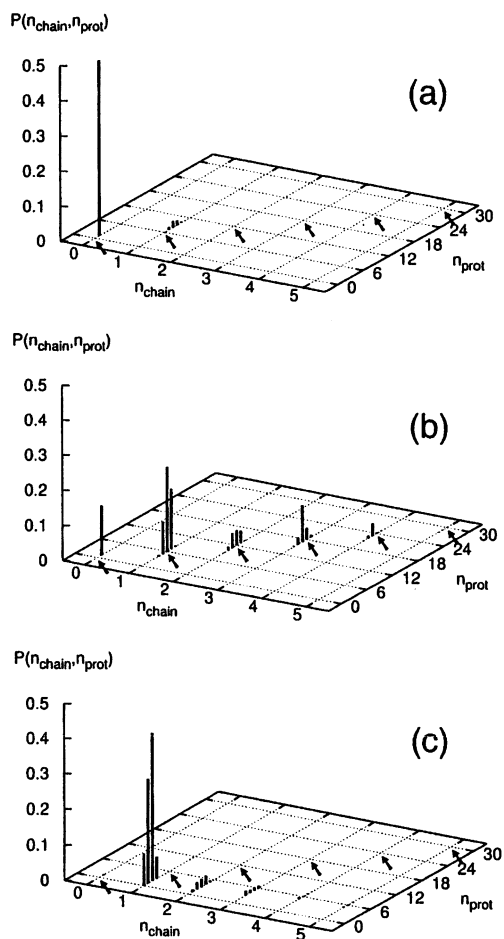
Figure 4. Probability $P(n_{chain},n_{prot})$ for clusters consisting of n_{chain} polyelectrolytes and n_{prot} proteins for system 1 with (a) $\beta = 0.2$, (b) 1, and (c) 4. The arrows indicate neutral cluster compositions. In (a), the large bar for $n_{chain} = 0$ and $n_{prot} = 1$ has been truncated [$P(0,1) = 0.96$]. The cluster criterion $r < R_{prot} + R_{bead} + 5$ Å is used as described in the text.

different quantity. For example, the probability of finding a protein in a cluster containing n_{prot} proteins with an unspecified number of polyelectrolyte chains is given by $n_{prot} \sum_{nchain} P(n_{chain},n_{prot})/\sum_{nchain} \sum_{nprot} n_{prot} P(n_{chain},n_{prot})$. Here, the probabilities are weighted with n_{prot}. Thus, the probability for a protein to appear in a large cluster is higher than the probability of the corresponding cluster.

Figure 4 shows the probabilities $P(n_{chain},n_{prot})$ for system 1 at $\beta = 0.2$, 1, and 4. In Figure 4, the arrows denote the cluster composition at which the clusters are electroneutral ($n_{prot} = 6n_{chain}$).

At $\beta = 0.2$, the solution contains $N_{chain} = 1$ polyelectrolyte chain and $N_{prot} = 30$ proteins with a 5-fold excess of protein charge. Figure 4a shows that the system is dominated by clusters composed of one polyelectrolyte chain and between 7 and 9 proteins and by uncomplexed (free) proteins. The polyelectrolyte-containing clusters possess the same net charge as the proteins and are hence overcharged by the proteins. Thus, the overcharging of a polyelectrolyte by proteins in a solution with excess of protein charges becomes $\approx 40\%$ of the polyelectrolyte charge.

Figure 4b displays the distribution of cluster compositions at the charge ratio $\beta = 1$. Here, the solution contains 5 polyelectrolyte chains and 30 proteins. There is a considerable variation of the cluster composition ranging from a substantial
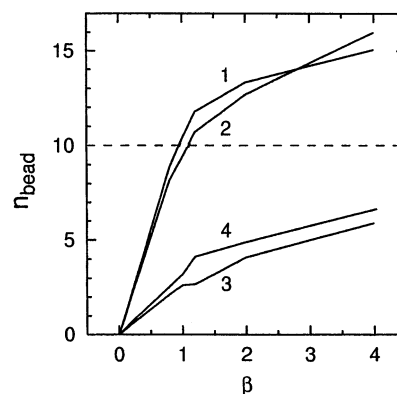

Figure 5. Number of polyelectrolyte beads n_{bead} within a distance $r = R_{prot} + R_{bead} + 5$ Å from the center of a protein as a function of the charge ratio β for indicated system. The dashed line denotes the amount of beads required to neutralize the protein net charge.

probability of forming large complexes involving 4 chains and 23 proteins to free proteins. From the data, we extract that the probability of finding a protein in a cluster involving 3 or more polyelectrolyte chains amounts to $\approx 45\%$. Noticeable is that clusters formed are neutral or near neutral (see arrows). Moreover, clusters involving one polyelectrolyte chain are more likely to be overcharged than undercharged, whereas clusters involving 3 or 4 chains tend to be undercharged.

Finally, at the charge ratio $\beta = 4$, Figure 4c shows that clusters formed contain again fewer macromolecules. There is a dominance of clusters containing polyelectrolyte chains with one or two proteins and these clusters are thus negatively charged. The solution contains no free proteins.

The overcharging of a polyelectrolyte in a solution with excess of macroions has previously been studied theoretically. Nguyen and Shklovskii[23] found a considerable overcharging, which first was increased and then decreased as the ionic strength was raised, whereas Schiessel et al.[44] predicted only a moderate deviation from a neutral cluster. Moreover, Jonsson and Linse studied similar systems and observed an overcharging of the polyelectrolyte by complexed charged spheres by 50–100%[27] or 50–70%,[28] depending on macroion charge and the polyelectrolyte rigidity. Hence, the obtained overcharging by $\approx 40\%$ at $\beta = 0.2$ is in line with previous and related simulations.

4.3 Accumulation of Polyelectrolyte Beads Near Proteins. The number of polyelectrolyte beads within the distance $r = R_{prot} + R_{bead} + 5$ Å from the center of the proteins, denoted by n_{bead}, has been used to characterize the accumulation of polyelectrolyte beads near a protein. In the evaluation of n_{bead}, averages are made over all proteins. Again the results do not depend critically on the selected distance.

Figure 5 shows n_{bead} as a function of the charge ratio β for the four systems. Generally, the number of nearby beads increases as β is increased, since more polyelectrolyte beads are available in the system. The increase is essentially linear up to charge equivalence ($\beta = 1$), and n_{bead} display a slower growth when polyelectrolyte charges are in excess ($\beta > 1$). Thus, despite that fewer beads are shared by several proteins at $\beta > 1$ (smaller clusters), n_{bead} increase when the polyelectrolyte charges becomes in excess.

(44) Schiessel, H.; Bruinsma, R. F.; Gelbart, W. M. *J. Chem. Phys.* **2001**, *115*, 7245−7252.
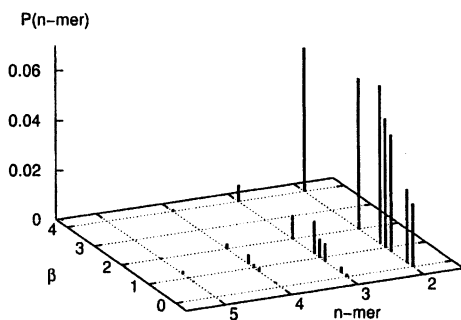
Figure 6. Probability $P(n\text{-mer})$ of a protein oligomer of size n for system 4 at different β. The criterion for protein oligorimerization is described in the text. The probabilities of the monomers are not shown.

At $\beta > 1$, systems 1 and 2 display $n_{\text{bead}} > 10$, indicating that the absolute charge of the nearby beads exceeds that of the protein. Moreover, according to Figure 5, the overcharging of a protein by polyelectrolyte beads in a solution containing a large excess of polyelectrolyte charges ($\beta \gg 1$) is $\approx$50% $-$ 60%. System 2 possessing the shorter polyelectrolyte displays a somewhat smaller amount of nearby beads (except for $\beta = 4$) as compared to system 1, which is consistent with the weaker cluster formation shown in Figure 3.

Systems 3 and 4 display a much smaller number of nearby beads as compared to systems 1 and 2 and n_{bead} does not reach 10 and hence in these systems the proteins never become overcharged. This trend is consistent with the weaker tendency for forming clusters as discussed in connection with Figure 3, which of course both originate from the weaker protein$-$ polyelectrolyte attraction owing to the larger electrostatic screening. Finally, the comparison of n_{bead} between system 3 and 4 confirms that the addition of a nonelectrostatic protein$-$ protein attraction leads to a stronger protein$-$polyelectrolyte attraction, as already concluded.

4.4 Protein Oligomers. In aqueous solution, lysozyme associates and forms dimers and to some extent trimers.[45] In a previous simulation study,[32] we have predicted that lysozyme oligomerization is favored by increasing protein concentration, decreasing protein net charge, and increasing electrolyte concentration, in agreement with experimental observations.

The propensity of lysozyme to form oligomers in polyelectrolyte-containing solution has also been examined. Two proteins were considered to belong to the same n-mer if they are "connected" directly or indirectly through one or several proteins. Two proteins are directly connected if $r_{\text{prot,prot}} < 2R_{\text{prot}} + 4$ Å. We have thus adopted the distance criterion of 4 Å for formation of a protein n-mer as in our previous study,[32] which gave a good agreement with experimental results regarding values of protein association constants.

Figure 6 shows the probability of forming an n-mer at different β for system 4. Throughout, the most probable n-mer is the monomer. In addition to monomers, dimers and to some extent trimers are predicted to appear in a polyelectrolyte-free lysozyme solution. As the polyelectrolyte is added, the probability of forming protein oligomers increases. At $\beta = 1$ to 2, the probability of dimers and trimers are substantially enhanced. Also tetramers are present, and the probability for a protein to appear in a tetramer is $\approx$1%. The enhanced formation of protein
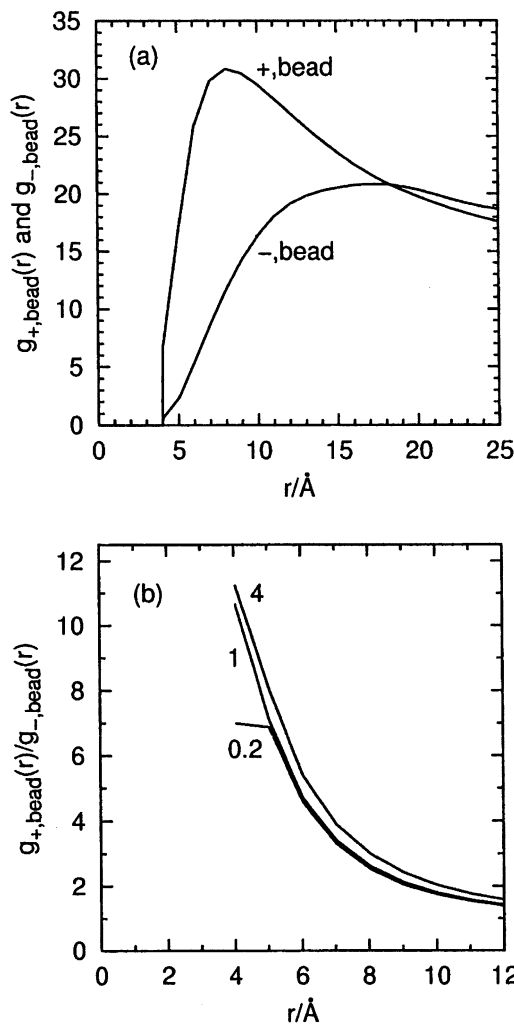
(45) Wang, F.; Hayter, J.; Wilson, L. J. *Acta Crystallogr., D Biol. Crystallogr.* **1996**, *D52*, 901$-$908.

Figure 7. (a) Protein charge-polyelectrolyte bead radial distribution functions $g_{+,\text{bead}}(r)$ and $g_{-,\text{bead}}(r)$ for system 1 at $\beta = 1$ and (b) their ratio $g_{+,\text{bead}}(r)/g_{-,\text{bead}}(r)$ for system 1 at indicated β.

oligomers and the increase in the local protein density near a protein (see Figure 3d) are of course related. At $\beta = 4$, the probability of forming oligomers is reduced as compared to $\beta = 2$.

Finally, it is anticipated that the enhancement of the formation of lysozyme oligomers is accelerated at lower ionic strength where the stronger electrostatic protein-polyelectrolyte attraction leads to larger clusters.

4.5 Charge Matching. Within our description, the proteins carry both positive and negative charges. These charges are positioned in an irregular pattern (see Figure 1 of ref 32) and follow closely the crystal structure of lysozyme. Due to the unequal electrostatic interaction with the negatively charged polyelectrolyte beads, it is conceivable that the local density of beads near positive and negative protein charges will differ. Of course, such charge correlations do not appear when the protein charge distribution is represented by a single central charge.

This degree of charge matching is illustrated in Figure 7a displaying the rdf between positive protein charges and polyelectrolyte beads ($g_{+,\text{bead}}$) and between negative protein charges and polyelectrolyte beads ($g_{-,\text{bead}}$) for system 1 at $\beta = 1$. Both rdf's display a maximum at short separation and a decay smoothly to zero at contact separation due to the accumulation of the beads near the protein and the entropic repulsion between
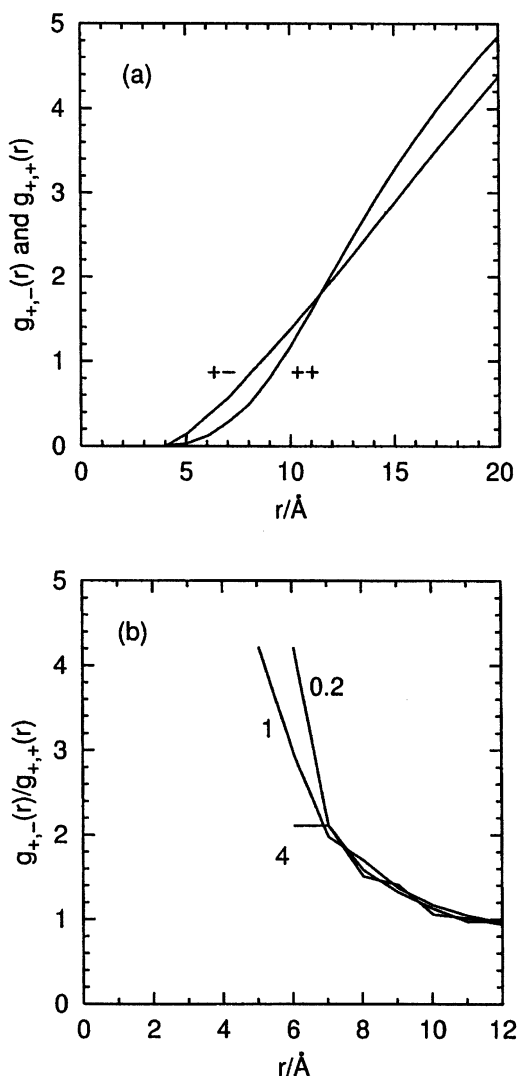
Figure 8. (a) Protein charge-protein charge radial distribution functions $g_{+,-}(r)$ and $g_{+,+}(r)$ for system 1 at $\beta = 1$ and (b) their ratio $g_{+,-}(r)/g_{+,+}(r)$ for system 1 at indicated β.

a polymer and an extended hard surface at short separation. Moreover, $g_{+,\text{bead}}$ display a larger maximum shifted to shorter separation as compared to $g_{-,\text{bead}}$, signaling that a substantial preferential arrangement of the beads near the protein. However, beyond $r \approx 40$ Å ($2R_{\text{prot}}$) the two rdf's become equal (not shown). (The unusual large value of the rdf at short separation ($g(r) \gg 1$) arises from the inhomogeneous distribution of the macromolecules at this condition, see Figure 2, middle.)

The charge correlations as depicted by the ratio $g_{+,\text{bead}}(r)/g_{-,\text{bead}}(r)$ are given in Figure 7b for system 1 at $\beta = 0.2$, 1, and 4. This charge ratio varies smoothly in the vicinity of the protein charges, and it is only weakly dependent on the stoichiometric charge ratio β, demonstrating that the charge correlations are essentially a local effect. At protein charge-bead contact, the bead density is ca. 10 times larger for positive protein charges as compared to negative ones. The degree of charge matching decreases as the ionic strength is increased (data not shown).

Similar charge matching between charges localized on different proteins is also expected. Again employing system 1 at $\beta = 1$, Figure 8a displays rdf's between unlike protein charges $g_{+,-}(r)$, and between positive protein charges $g_{+,+}(r)$. Both these rdf's display maximums at $r \approx 40$ Å (cf. Figure 3a displaying

the center-to-center rdf). However, focusing on the rdf's at short separations, there is indeed a positive correlation between unlike charges between $r = 4$ and 10.5 Å. Thus, despite that nearby proteins display charge correlations with respect to complexing polyelectrolyte beads, pairs of proteins are still able to establish charge correlations with respect to each other. In fact, similar degree of charge correlations was found in polyelectrolyte-free solution (see Figure 8a of ref 32).

Finally, Figure 8b shows the ratio $g_{+,-}(r)/g_{+,+}(r)$ for system 1 at different β. As for the protein charge−polyelectrolyte bead pairs, the protein charge−protein charge correlations appear to be insensitive to the polyelectrolyte concentration and the subsequent variation of protein environments (cf. Figure 2).

Thus, the presence of both positive and negative protein charges enables short-range spatial correlations. The charged polyelectrolyte beads are locally unevenly distributed around the protein and there appears to be a sufficiently degree of flexibility enabling the charge−charge correlations, appearing between two nearby proteins in absence of polyelectrolyte, to remain when polyelectrolyte is present.

5. Summary

On the basis of Monte Carlo simulations of a model system representing an aqueous protein solution with variable concentration of oppositely charged polyelectrolyte, the propensity of forming protein−polyelectrolyte clusters, the composition of the clusters, and to some extent the local structure of the clusters have been investigated. Different polyelectrolyte length, ionic strength of the solution, and protein models, of which one was constructed to represent lysozyme, have been employed.

The strong attractive electrostatic interaction between the protein and the polyelectrolyte established a strong association between protein and polyelectrolyte beads. In the system with the largest electrostatic coupling, there was an extensive cluster formation at stoichiometric charge ratio. In excess of polyelectrolyte, a redissolution appeared but still the proteins were attached to polyelectrolytes.

As the polyelectrolyte chains were shortened, the same scenario appeared, but the protein−polyelectrolyte association became weaker making the clusters less extended. At a 10-fold increase of the ionic strength, the electrostatic interaction becomes sufficiently screened impeding an extended cluster formation. Nevertheless, the additional inclusion of a nonelectrostatic protein−protein attraction, making the protein model representing lysozyme, some of the previous tendency of cluster formation was regained. Thus, nonelectrostatic attraction bringing proteins together promotes the protein−polyelectrolyte association and facility protein−polyelectrolyte cluster formation.

In the system with the strongest electrostatic interaction, cluster analyses showed that in a solution with an excess of proteins, polyelectrolyte complexes proteins such that the polyelectrolyte becomes overcharged by the protein charges. Similarly, in a solution with excess of polyelectrolyte, a protein forms a complex with a polyelectrolyte such that the protein charge become overcharged by nearby polyelectrolyte charges. In both cases, we count charges within 5 Å from hard-sphere contact.

In polyelectrolyte-free solution, lysozyme tends to form small oligomers. It was shown that this ability is enhanced in solutions containing oppositely charged polyelectrolytes.

Finally, on short distances substantial spatial charge correlations appeared displaying that the local density of polyelectrolyte beads near positive and negative protein charges differs.

JA020935A